Mnb/Dyrk1A Phosphorylation Regulates the Interaction of Dynamin 1 with SH3 Domain-Containing Proteins†

Yu Huang,‡,§ Mo-Chou Chen-Hwang,‡ Georgia Dolios,|| Noriko Murakami,‡ Júlio C. Padovan,⊥ Rong Wang,|| and Yu-Wen Hwang*,‡,§

Molecular Biology Department, New York State Institute for Basic Research in Developmental Disabilities, Staten Island, New York 10314, CSI/IBR Center for Developmental Neuroscience and Graduate Program in Biology, City University of New York, New York, New York 10016, Department of Human Genetics, Mount Sinai School of Medicine, New York, New York 10029, and Laboratory for Mass Spectrometry and Gaseous Chemistry, The Rockefeller University, New York, New York 10021

Received November 17, 2003; Revised Manuscript Received June 4, 2004

ABSTRACT: Mnb/Dyrk1A is a proline-directed serine/threonine kinase implicated in Down's syndrome. Mnb/Dyrk1A was shown to phosphorylate dynamin 1 and alter its interactions with several SH3 domain-containing endocytic accessory proteins. To determine the mechanism of regulation, we mapped the Mnb/Dyrk1A phosphorylation sites in dynamin 1. Using a combination of deletion mutants and synthetic peptides, three potential Mnb/Dyrk1A phosphorylation sites (S778, S795, and S857) were first identified. Phosphorylation at S795 and S857 was confirmed in full-length dynamin 1, and S857 was subsequently determined to be the major Mnb/Dyrk1A phosphorylation site *in vitro*. Phosphorylation at S857 was demonstrated to be the basis for altering the binding of dynamin 1 to amphiphysin 1 and Grb 2 by site-directed mutants mimicking phosphorylation. Furthermore, S857 of dynamin 1 is phosphorylated by the endogenous kinase in brain extracts and in PC12 cells. In PC12 cells, the state of S857 phosphorylation is dependent on membrane potentials. These results suggest that S857 phosphorylation is a physiological event, which regulates the binding of dynamin 1 to SH3 domain-containing proteins. Since S857 is unique to dynamin 1xa isoforms, Mnb/Dyrk1A regulation of dynamin 1 is expected to be specific to these spliced variants.

Dynamin 1 is known to participate in clathrin-mediated endocytic synaptic vesicle recycling (for a review, see ref *1*). This protein assembles around the neck of invaginated clathrin-coated pits and appears to function as a chemomechanical enzyme that severs the emerging coated vesicles from the cell membrane. Dynamin 1 binds and hydrolyzes GTP through the highly conserved GTPase domain in its N-terminus. Dynamin 1 also contains a pleckstrin domain for binding lipids and a proline-rich domain (PRD)[1] for interacting with SH3 domain-containing proteins, such as many endocytic accessory proteins (*2*, *3*). The interactions of dynamin 1 with endocytic accessory proteins are generally considered to be required for recruiting dynamin 1 into functional complexes.

Dynamin 1 is a phosphoprotein, and the state of its phosphorylation depends on membrane potentials (*4*, *5*). The protein is phosphorylated in resting cells and can undergo rapid dephosphorylation upon membrane depolarization (*4*, *5*), an event coinciding with the onset of endocytosis. Phosphorylation was subsequently shown to inhibit the binding of dynamin 1 with amphiphysin, an endocytic accessory protein (*6*). Several kinases are known to phosphorylate dynamin 1 (*7*−*10*), and recently, Cdk5 was implicated as a potential dynamin 1 kinase, which regulates the interactions of dynamin 1 with amphiphysin (*10*).

Dynamin 1 was also shown to be a minibrain kinase/dual-specificity Yak 1-related kinase 1A (Mnb/Dyrk1A) substrate (*11*, *12*). The *Mnb* was originally identified in *Drosophila* as a gene required for the proliferation of neuroblasts during postembryonic neurogenesis (*13*). Mutation in the gene causes a reduction in the brain size of adult flies and produces distinct memory and behavioral defects (*13*). The human ortholog of the *Drosophila Mnb* gene, Dyrk1A, is localized

† This work is supported in part by NIH Grants HD38295 (Y.-W.H.) and CA88325 (R.W.) and by the New York State Office of Mental Retardation and Developmental Disabilities. Part of the MS analysis was conducted at the National Resource for the Mass Spectrometric Analysis of Biological Macromolecules at The Rockefeller University (NIH Grant RR-00862).

* To whom correspondence should be addressed: Molecular Biology Department, New York State Institute for Basic Research in Developmental Disabilities, 1050 Forest Hill Rd., Staten Island, NY 10314. Telephone: (718) 494-5337. Fax: (718) 494-5905. E-mail: hwang@mail.csi.cuny.edu.

‡ New York State Institute for Basic Research in Developmental Disabilities.

§ City University of New York.

|| Mount Sinai School of Medicine.

⊥ The Rockefeller University.

[1] Abbreviations: BTE, brain Triton X-100 extract; ELISA, enzyme-linked immunosorbent assay; GST, glutathione *S*-transferase; IP, immunoprecipitation; IPTG, isopropyl β-thiogalactoside; MS, mass spectrometry; Mnb/Dyrk1A, minibrain kinase/dual-specificity Yak1-related kinase 1A; PAGE, polyacrylamide gel electrophoresis; PBS, phosphate-buffered saline; PCR, polymerase chain reaction; PKC-M, catalytic domain, protein kinase C; PAA, phospho-amino acids; PRD, proline-rich domain; PS, phosphoserine; PT, phosphothreonine; PY, phosphotyrosine; SH3, src homology domain 3.

10.1021/bi036060+ CCC: $27.50
Published on Web 07/14/2004

Table 1: Phosphorylation of GST Fusion Clones Containing Different Regions of the Dynamin 1xa PRD Fragment

clone	GST fusion clone sequence	Mnb/Dyrk1A phosphorylation
P1	MRS^{774}PTS^{777}S^{778}PTP	yes
P2	MRPGS^{795}RGP	yes
P3	MPPAGS^{807}ALGG	no
P4	MPPVPS^{817}RPGA	no
P5	MRPGAS^{822}PDPF	no
P6	MPPQVPS^{834}RPNR	no
P7	MPGVPS^{845}RS^{847}GQA	no
P8	MGQAS^{851}PS^{853}RPE	no
P9	MRPES^{857}PRPP	yes
S777A	MRSPTA^{777}S^{778}PTP	yes
S778A	MRSPTS^{777}A^{778}PTP	no

to the Down's syndrome critical region of chromosome 21 (*14*−*18*). The level of expression of Mnb/Dyrk1A is elevated in patients with Down's syndrome (*19*, *20*), and Mnb/Dyrk1A overexpression appears to be the foundation for motor, cognitive, and memory abnormalities in transgenic mice (*21*, *22*).

When dynamin 1 is phosphorylated with Mnb/Dyrk1A at low kinase concentrations, the phosphorylation inhibits the binding of dynamin 1 to amphiphysin 1 (*12*). This result implicates Mnb/Dyrk1A as a potential dynamin 1 kinase whose activity modulates the interaction of dynamin 1 with amphiphysin (*6*). However, at higher kinase concentrations, Mnb/Dyrk1A phosphorylation promotes rather than inhibits the binding of dynamin 1 to amphiphysin 1 (*12*). This biphasic phenomenon appears to be related to the stoichiometry of dynamin 1 phosphorylation (*12*). Apparently, Mnb/Dyrk1A phosphorylates multiple dynamin 1 sites, which produces complex biochemical consequences. To elucidate the molecular basis underlying the effects of Mnb/Dyrk1A on the interaction of dynamin 1 with SH3 domains, the phosphorylation sites were determined in this study. Dynamin 1 contains two alternatively spliced sites, one at the middle of the protein (two splicing forms) and the other at the C-terminus (four splicing forms), which when combined give rise to eight splicing variants (*23*, *24*). Whenever necessary, the notation dynamin 1(a,b)(a,b,c,d) will be used to differentiate spliced variants.

MATERIALS AND METHODS

Clone Construction. C-Terminally truncated mutants of GST−dynamin 1aa clones (C3, C4, and C5) were constructed by PCR from rat dynamin 1aa vector pCMV96-7 (*23*) using oligonucleotides CCTCTCGAGTCAGGAGGGCACGGGGGGAGCCCCCCC, CCTCTCGAGTCAGGCTGGGGGCACGGCGGGGGCTCG, and CCTCTCGAGTCATCCGGCCGGTACGCTCTGCACCTG, respectively, as the 3′ end primer and TCTCATCGATGGGCAACCGCGGCATGGAAGACCTC as the 5′ end primer. The resulting amplicons were digested with *Cla*I and *Xho*I (introduced by 5′ and 3′ primers, respectively) and then cloned into the *Cla*I and *Xho*I sites of the pGEX vector as described previously (*25*). To construct GST fusion clones containing dynamin 1xa PRD fragments, a set of oligonucleotide linkers, each specific for the desired amino acid sequence, were synthesized (Table 1) and cloned into the pGEX vector as described above. The high GC content in the 3′ end region of the dynamin 1xa gene has hampered the construction of the S857 mutations by oligonucleotide site-directed mutagenesis. Therefore, the region from the *Apa*I site (residues 797 and 798) to the 3′ end of the rat dynamin 1xa gene (214 nucleotides) was synthesized. The synthesized DNA incorporates an *Xba*I (at residues 853 and 854) and an *Xho*I (immediately followed the stop codon) sites for mutant construction and cloning. This fragment was ligated together with the *Kpn*I−*Apa*I dynamin 1aa fragment (from the start codon to residues 797 and 798) obtained from pCMV96-7 into a modified plasmid vector pND1 (*25*). A hemagglutinin (HA) tag was then added to the N-terminus of dynamin 1aa by PCR to produce the pNDHA-dynamin 1aa clone. Mutants were subsequently constructed on pNDHA-dynamin 1aa by fragment replacement utilizing the unique *Sma*I−*Apa*I (for the S795E mutation) and *Xba*I−*Xho*I sites (for the S857E mutation). Subsequently, mammalian expression vectors, pcDY1aa, were assembled by inserting HA-dynamin 1aa clones into the *Eco*RI−*Xho*I sites of vector pcDNA3 (Invitrogen). The following approach was used to construct mammalian vector pcMnb for expressing full-length Mnb/Dyrk1A. First, vector pMnb was constructed by inserting the Mnb/Dyrk1A fragment from the GST fusion vector (*12*) into the T7 RNA polymerase vector pND1 through *Cla*I and *Xho*I sites as described previously (*26*). Vector pRHC-Mnb was created by replacing the *Eco*RI (in vector pND 1)−*Sph*I (codon 10 of the Mnb/Dyrk1A gene) fragment in vector pMnb with an oligonucleotide linker (AATTCAAGCTTATCGATGCATACAGGAGGAGAGACTTCAGCATG). This oligonucleotide restored the N-terminal Mnb/Dyrk1A gene and added a *Hin*dIII site at the 5′ untranslated region. Subsequently, the Mnb/Dyrk1A gene was spliced into vector pcDNA3 (Invitrogen) through the *Hin*dIII−*Xho*I sites. The kinase-deficient mutant harboring the Y319F and Y321F substitutions was described previously (*12*).

Table 2: Sequence and Mnb/Dyrk1A Phosphorylation of Dynatides[a]

peptide	sequence	K_m (μM)	k_{cat} (min^{-1})
dynatide 1	RRSPTSS^{778}PTPQRRC	230	1.27
dynatide 2	RPARPGS^{795}RGPAPGC	175	4.20
dynatide 3	RASPSRPES^{857}PRPPC	63	20.7

[a] Dynatide 1 contains the exact dynamin 1xa sequence except for the C-terminal cysteine residue (Figure 1). For both dynatides 2 and 3, an extra arginine was added to the N-terminus in addition to the C-terminal cysteine residue to ensure tight phosphocellulose binding. The added arginine and cysteine are beyond the core sequence (P−3 to P+1) required for phosphorylation (*33*).

Kinase Assays. The solution and solid-phase Mnb/Dyrk1A phosphorylation was performed as described previously (*12*). The activity of Mnb/Dyrk1A was determined in a 30 μL reaction mixture containing a kinase buffer [25 mM HEPES (pH 7.5), 100 mM NaCl, 5 mM $MgCl_2$, and 5 mM $MnCl_2$], 1 μg of dynatide 3 (Table 2 and Figure 1B), 2 μCi of [γ-^{32}P]-ATP (specific activity of 1.33 Ci/mmol), and 0.1 μg of Mnb/Dyrk1A. The reaction was allowed to proceed at 30 °C for 10 min. A 5 μL aliquot of the reaction mixture was withdrawn at the end of the incubation, and the extent of ^{32}P incorporation was determined by P81 phosphocellulose membrane binding as described previously (*27*). Parallel experiments with dynatide 3 alone as well as Mnb/Dyrk1A alone were similarly performed and used for background subtraction. One unit of Mnb/Dyrk1A is defined as the amount of kinase capable of catalyzing 1 pmol of phosphate

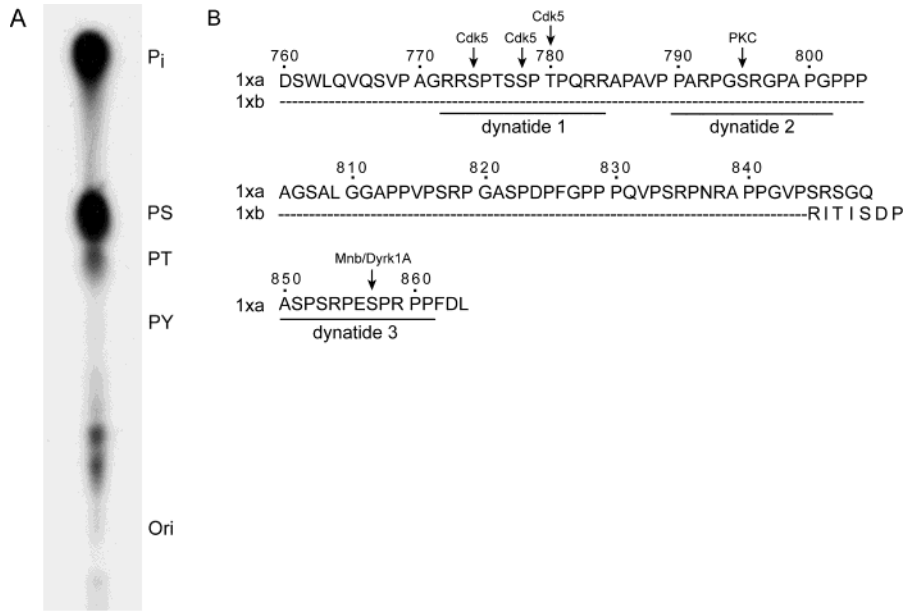

FIGURE 1: PAA analysis of phosphorylated dynamin 1 (A) and the sequence of dynamin 1xa PRD (B). (A) Dynamin 1 (1 μg) was phosphorylated by Mnb/Dyrk1A (2 units) in the presence of [^{32}P]ATP and then subjected to PAA analysis as described in Materials and Methods. P_i is free phosphate and Ori the origin. (B) PRD sequence of dynamin 1xa and 1xb variants. Residues in PRD known to be phosphorylated are S774 (Cdk5) (*9*), S778 (Cdk5) (*9*), T780 (Cdk5) (*10*), and S795 (PKC) (*34*). S857 was identified as the major Mnb/Dyrk1A phosphorylation site in this study. Dynatide sequences (Table 2) are marked.

incorporation into dynatide 3 per minute. The activity of purified Mnb/Dyrk1A is usually around 20−40 units/μg of protein. Kinetic constants for dynatide phosphorylation were determined from a series of reaction mixtures containing 5−60 μM peptide substrate as described previously (*12*). The data reported in the study were the average of three independent experiments. Phosphorylation of dynamin 1 by PKC-M (protein kinase C catalytic subunit) was performed by incubating 1 μg of dynamin 1 with 10 ng of PKC-M (EMD Biosciences, Inc.) in a 30 μL reaction mixture for 30 min as specified by the supplier.

Antibodies and Immunological Assays. Goat polyclonal anti-dynamin 1 antibody (C-16) and anti-dynamin 1 PS795 antibody (p-Dynamin I) were purchased from Santa Cruz Biotechnology. Mouse monoclonal anti-dynamin 1 antibody (Hudy-1) was obtained from Upstate Biotechnology. Mouse monoclonal antibody, 3D3, specific to PS857 dynamin 1 was produced by following a standard production protocol (*28*). Antigen, conjugated Mnb/Dyrk1A-phosphorylated dynatide 3, was prepared as described below. First, dynatide 3 (1 mg) was exhaustively phosphorylated with three successions of 2000 units of Mnb/Dyrk1A, each for 90 min. Upon completion, the reaction mixture was adjusted to pH 4 with acetic acid and incubated on ice for 20 min to precipitate Mnb/Dyrk1A, which was subsequently removed by centrifugation (12000*g* for 20 min). Phosphorylated dynatides were then treated with tributylphosphine (*29*) and conjugated to 2 mg of activated Supercarrier (Pierce). Antibody clones were screened against control and Mnb/Dyrk1A-phosphorylated dynatide 3 with an ELISA. Clone 3D3 was selected on the basis of its selectivity for Mnb/Dyrk1A-phosphorylated over control dynatide 3 (see Figure 6). Mouse monoclonal anti-Mnb/Dyrk1A antibody 7F3 was also produced as described previously (*30*). Immunoblotting was performed as previously described (*12*). The ELISA was carried out by assessing the turnover of *p*-nitrophenyl phosphate similarly as described previously (*28*). Immobilized antibody (Hudy-1 or C-16) was prepared by incubating 50 μL (bed volume) of washed Ultralink protein A/G (Pierce) with 10 μg of antibody for 2 h at 4 °C. Coated beads were then washed twice with cold PBST (PBS and 0.25% Tween-20), resuspended, and stored in 250 μL of PBSTA at 4 °C until they were used.

PAA Analysis. ^{32}P-labeled dynamin 1 was prepared by phosphorylating 1 μg of dynamin 1 with either 2 or 24 units of Mnb/Dyrk1A in the presence of [γ-^{32}P]ATP as described above. Dynamin was immunoprecipitated (IP) in 200 μL of a mixture with 50 μL of immobilized Hudy-1 for 2 h at 4 °C. After being washed, labeled dynamin was eluted from resins with 0.1 N HCl. Eluted proteins were hydrolyzed under vacuum at 110 °C for 2 h in the presence of 6 N HCl, mixed with 3 μg each of phospho-amino acid standards, and then subjected to high-voltage electrophoresis on silica gel 60 plates (Alltech) according to the method of Hunter and Sefton (*31*). PAA standards and the labeled amino acid were detected by ninhydrin spray and autoradiography, respectively.

Identification of the Phosphorylation Site in Dynatides. Dynatides 1 and 3 were phosphorylated with Mnb/Dyrk1A in the presence of [γ-^{32}P]ATP as described above. Phosphorylated dynatides were then purified with a Sep-Pak cartridge (Waters), immobilized onto a Sequelon AA disk (Millipore), and subjected to manual Edman degradation according to the method of Sullivan and Wong (*32*). Radioactivity released in each degradation cycle was measured in a liquid scintillation counter.

Identification of the Phosphorylation Site in Dynamin by Mass Spectrometry. The phosphorylated dynamin to be analyzed was purified by SDS−PAGE. The dynamin band was visualized by Coomassie Blue staining, excised, and further destained with 100 μL of acetonitrile (ACN) and 50 mM NH_4HCO_3 (45:55, v/v) at 4 °C for 1.5 h. Subsequently, proteins were reduced with 10 mM tris(2-carboxyethyl)-phosphine hydrochloride (in 50 mM NH_4HCO_3) at pH 7.5−

8.0 and 37 °C for 30 min, alkylated with 50 mM iodoacetamide (in 50 mM NH_4HCO_3) in the dark at room temperature for 1 h, and digested with trypsin (Roche) *in situ* overnight. The resulting tryptic peptides were extracted using POROS 20 R2 beads (10 μL of a 1:20 dilution) in the presence of 5% formic acid and 0.2% trifluoroacetic acid (TFA) overnight. The tryptic peptides were eluted sequentially with 20 μL of 30 and 75% ACN containing 0.1% TFA using C18 Zip-tips and lyophilized.

The dried tryptic peptides were resuspended in 4 μL of a mixing solvent composed of water and methanol (3:2, v/v) containing 0.5% acetic acid and 0.01% TFA followed by a 2.5-fold dilution with the same solvent before analysis. Phosphorylation modification of dynamin was initially identified by MALDI-TOF mass spectrometry. To perform the analysis, the tryptic peptide solution (0.5 μL) was mixed with 0.5 μL of a saturated α-cyano-4-hydroxycinnamic acid matrix solution in water and ACN (2:1, v/v) containing 0.1% TFA and spotted onto the MALDI target plate. All spectra were acquired using a Voyager-DE STR MALDI time-of-flight mass spectrometer (Applied Biosystems) operating in delayed extraction linear mode and averaged from 256 individual laser shots. Spectra were calibrated using the trypsin autodigest fragment and analyzed using M/Z and Paws against the dynamin amino acid sequence for phosphorylation identification.

Phosphorylation identified by MALDI-TOF MS was confirmed by LC-ESI tandem mass analysis. LC−MS/MS of the derivatized peptides was performed by a capillary HPLC system (Amersham Biosciences) coupled directly to an LCQ^{Deca} ion trap mass spectrometer (Thermo Finnigan). The diluted tryptic peptide solution (2 μL) was separated by a Magic reverse-phase C-18 capillary HPLC column (0.2 mm × 50 mm, 5 μm, 100 Å) (Michrom Bioresources, Inc.) with a 0 to 100% methanol (in water) gradient containing 0.01% TFA and 0.5% acetic acid. The ion trap mass spectrometer was operated in data-dependent MS/MS mode with parent masses setting at *m*/*z* values of doubly and triply protonated phosphorylated dynamin peptides.

Dynamin 1 Mutant Production and Binding Assay. Cos7 cells (3×10^6 cells per 60 mm dish) were maintained in DMEM supplemented with 10% fetal calf serum and transfected with pcDY1aa clones by using Lipofectamine 2000 (Invitrogen) as suggested by the supplier. Two days after the transfection, cells were lysed directly on the plate with 0. 4 mL of lysis buffer [50 mM Tris (pH 8.0), 150 mM NaCl, Roche protease inhibitor cocktail, and 1% NP-40] and centrifuged at 12000*g* for 5 min to remove cell debris. The relative levels of dynamin overexpression among different clones were estimated by immunoblotting using antibody Hudy-1. Binding assays were performed by mixing 300 μg of crude cell lysates (the expression level for all constructs is similar) with 0.6 nmol of immobilized GST fusion amphiphysin 1 SH3 domain or Grb 2 (full-length) as previously described (*12*). The precipitated HA-dynamin 1aa was detected by immunoblotting against Hudy-1.

BTE Preparation and Phosphorylation. The BTE was prepared from adult rat brains as described previously (*6*). For phosphorylation, the extract was incubated with 2 mM ATP, 4 μM cyclosporine, 0.2 μM okadaic acid, 1 mM sodium orthovandate, and 5 mM $MgCl_2$ at 30 °C for 40 min. A control was similarly prepared but without the addition of ATP and phosphatase inhibitors. At the end of the incubation, samples were boiled in SDS−PAGE loading buffer and subjected to immunoblotting against Hudy-1, 3D3, and p-Dynamin I. IP of dynamin 1 was performed by mixing 300 μL of brain extracts with Ultralink protein A/G-immobilized antibody C-16 (2.5 μg) for 16 h at 4 °C. After being washed with PBST, precipitated dynamin 1 was eluted by boiling in SDS−PAGE loading buffer and subjected to immunoblotting against antibodies Hudy-1 and 3D3.

Assessment of Dynamin 1 Phosphorylation in PC12 Cells. PC12 cells were maintained in F-12K medium (ATCC) supplemented with 5% fetal calf serum and 10% horse serum. The experiments were performed with 3×10^6 cells in a 60 mm dish by rinsing the cells once with KRH buffer [25 mM HEPES (pH 7.4), 125 mM NaCl, 4.8 mM KCl, 2.6 mM $CaCl_2$, 1.2 mM $MgSO_4$, and 5.6 mM glucose] and then incubating the cells in the same buffer for 1 h at 37 °C (polarization conditions). Depolarization was induced by the addition of 90 mM KCl to cell cultures for 5 min at 37 °C. Cell lysates were prepared directly on the plate by adding 0. 4 mL of lysis buffer supplemented with phosphatase inhibitors (0.2 μM okadaic acid, 4 μM cyclosporine, and 5 μM cypermethrin), followed by centrifugation at 12000*g* for 5 min to remove cell debris. Dynamin 1 was IP from 0.5 mg of lysate (total proteins) with immobilized antibody C-16 (2.5 μg) for 16 h at 4 °C and analyzed using antibodies 3D3, Hudy-1, and p-Dynamin I as described above. Antibody stripping was performed by incubating the blot in 0.2 M glycine (pH 2.5) for 1 h at room temperature. The level of S857 phosphorylation upon depolarization was determined by first correcting for the level of dynamin 1 (from Hudy-1 staining) and then normalized to that of polarized cells (set to 100%). Transfection of PC12 cells with the expression vector was performed in a manner similar to that described for dynamin 1 mutant expression. Twenty-four hours after the transfection, cells lysates were prepared in the presence of phosphatase inhibitors. S857 phosphorylation was assessed in IP dynamin with antibody 3D3 as described above. Mnb/Dyrk1A was detected in crude lysates using antibody 7F3 as described previously (*30*).

RESULTS

Mnb/Dyrk1A Phosphorylates Dynamin 1 Primarily on the Serine Residues. To facilitate the identification of Mnb/Dyrk1A target sites, the phospho-amino acid (PAA) profile was first determined. Purified rat brain dynamin 1 was phosphorylated by Mnb/Dyrk1A under native conditions, immunoprecipitated (IP), and subjected to PAA analysis (Figure 1A). Since Mnb/Dyrk1A undergoes autophosphorylation (*11*), IP was used to minimize the PAA contribution from kinase. The assay revealed that phosphorylated dynamin 1 consisted primarily of phosphoserine (PS) with trace amounts of phosphothreonine (PT) and no detectable phosphotyrosine (PY) (Figure 1A). This result supports the conclusion that Mnb/Dyrk1A functions as a serine/threonine kinase, and not as a dual-specificity kinase on dynamin 1. We have also performed PAA analysis on dynamin phosphorylated with a large dose of kinase, which is known to promote multiple phosphorylations (*12*). The resulting PAA profile was unchanged, indicating that the phosphorylation specificity of Mnb/Dyrk1A was independent of kinase concentration (data not shown). We started the search for

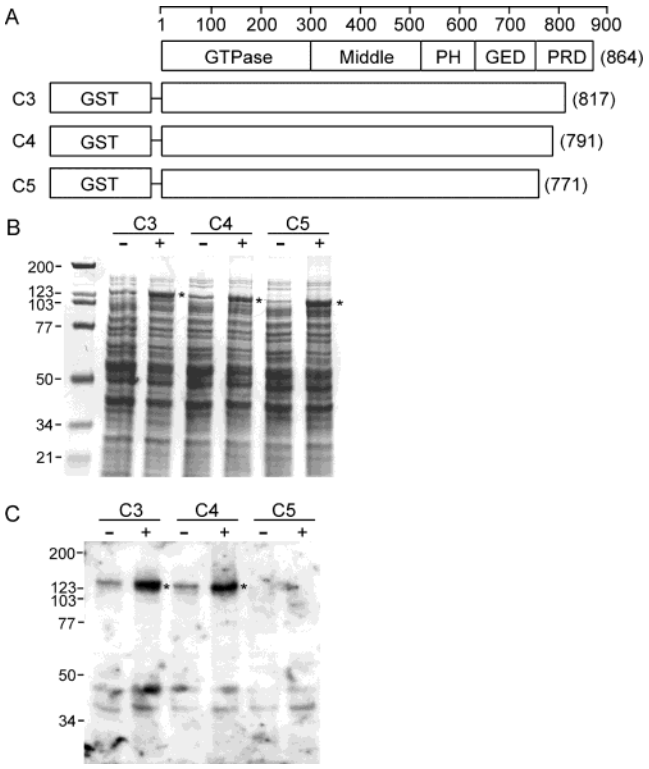

FIGURE 2: Expression and Mnb/Dyrk1A phosphorylation of GST−dynamin 1aa deletion mutants. (A) Structures of GST−dynamin 1aa deletion mutants. The structural domains are labeled as described previously (*1*). GTPase is the GTP hydrolysis domain, PH pleckstrin homology, GED the GTPase effector domain, and PRD the proline-rich domain. The numbers in parentheses indicate the last residue of each C-terminal end deletion clone. PRD deletion mutants were produced in *E. coli* by IPTG induction and subjected to Coomassie blue staining (B) and a solid-phase Mnb/Dyrk1A assay (C): (−) control and (+) IPTG-induced sample. The band corresponding to each deletion mutant is marked with an asterisk.

the phosphorylation sites from the dynamin 1 PRD because dynamin 1aa and 1ba (1xa in general) isoforms contain an Mnb/Dyrk1A-preferred sequence ^{854}RPESP^{858} in PRD (Figure 1B) (*33*). Since PS dominates in the PAA profile, our emphasis was placed on serine residues.

Identification of Three Mnb/Dryk1A Potential Sites at S778, S795, and S857 of Dynamin 1. To begin, a group of GST−dynamin 1aa truncated mutants were constructed by progressively removing amino acid residues from the C-terminus (Figure 2A). The proteins were expressed in *Escherichia coli* (Figure 2B) and subjected to the solid-phase Mnb/Dyrk1A assay (Figure 2C). A mutant lacking either 47 (clone C3) or 73 (clone C4) residues was phosphorylated by Mnb/Dyrk1A. In contrast, Mnb/Dyrk1A failed to phosphorylate clone C5, a mutant with 93 amino acids deleted. These results indicate that all Mnb/Dyrk1A phosphorylation sites are located within the last 93 residues of dynamin 1aa PRD.

The last 93 residues of rat dynamin 1xa include 13 serines (Figure 1B). To determine which serine could be phosphorylated, a group of GST fusion proteins, each containing 8−11 residues of PRD and 1−3 serines, were constructed and analyzed with the solid-phase Mnb/Dyrk1A assay. Together, these clones cover all 13 serine residues in the 93 target residues (Table 1). Results show that only clones P1, P2, and P9 could be phosphorylated by Mnb/Dyrk1A (Table 1). Phosphorylation of P2 and P9 implicates S795 and S857 as the potential phosphorylation sites, respectively. Clone P1 contains three serine residues. To pinpoint the target serine residue(s), two P1 variants, S777A and S778A, were further constructed and analyzed (Table 1). Via placement of an alanine at position S778 but not at S777, the extent of phosphorylation was reduced. The result suggests that S778 is the third potential kinase site.

Mnb/Dyrk1A Phosphorylates Synthetic Peptides Containing S778, S795, or S857. We subsequently verified the sites identified from GST clones in peptide substrates. Three peptides, dynatides (dynamin peptide) 1, 2, and 3, each encompassing one of the three potential phosphorylation sites were synthesized and analyzed (Figure 1B and Table 2). Mnb/Dyrk1A phosphorylates all three peptides. Dynatide 3, which matches the consensus Mnb/Dyrk1A phosphorylation sequence, was the best substrate among the three peptides (Table 2). The kinetic parameters are comparable to those of DYRKtide (*33*), a peptide substrate optimized for Mnb/Dyrk1A by combinatorial chemistry. Dynatide 2 was a weaker substrate than dynatide 3, and dynatide 1 was the weakest of the three. The trend of reactivity roughly follows the degree of similarity between the sequence of dynatides and the consensus phosphorylation sequence RPX(S/T)P (*33*).

Since dynatides 1 and 3 contain multiple serine residues, the position of the phosphorylated serine was subsequently determined by manual Edman degradation. It is clear that S778 is the phosphorylated site in dynatide 1 (Figure 3A). Neither S774, T776, S777, nor T780 was phosphorylated to a significant level. The same approach showed that S857 is the only phosphorylated residue in dynatide 3 (Figure 3B). These findings confirm that Mnb/Dyrk1A phosphorylates peptides and GST fusion proteins at the same site.

Verification of the Mnb/Dyrk1A Phosphorylation Sites in Intact Dynamin 1 by Mass Spectrometry (MS). To determine whether any of these potential sites were phosphorylated in intact protein, purified rat brain dynamin 1 was phosphorylated under native conditions, digested with trypsin, and then subjected to MS analysis. Tryptic peptides containing all three potential phosphorylation sites were identified in control dynamin 1 (Figure 4A, bottom panel). These peptides are S[774−784]R (or R[773−783]R) (*m*/*z* 1214.2) and R[773−784]R (*m*/*z* 1370.3) for S778, A[785−796]R (*m*/*z* 1175.2) and R[784−796]R (*m*/*z* 1332.2) for S795, and S[847−864]L (*m*/*z* 1926.0) for S857. The detection of the S[847−864]L peptide shows that our rat brain dynamin 1 preparation contains 1xa isoforms, which include 1aa and 1ba variants. Upon phosphorylation with a low concentration of kinase (2 units of kinase/μg of dynamin), a new peak corresponding to the phosphorylated S[847−864]L peptide (*m*/*z* 1926 + 80) appeared with a concomitant reduction in the level of the unphosphorylated peptide (Figure 4A, top panel). On the other hand, signals representing phosphorylated peptides of S778 or S795 were not detected (Figure 4A, top panel). The identity of the *m*/*z* 2006.1 peptide was subsequently determined by MS/MS. As shown in Figure 4B, the product ion spectrum of the precursor ion matched that of the phosphorylated peptide S[847−864]L. Specifically, the peak observed at *m*/*z* 954.1 corresponded to the doubly charged ion resulting from the loss of inorganic phosphate from the intact phosphorylated peptide. Several peaks corresponding to cleavages of peptide bonds were also detected, and their

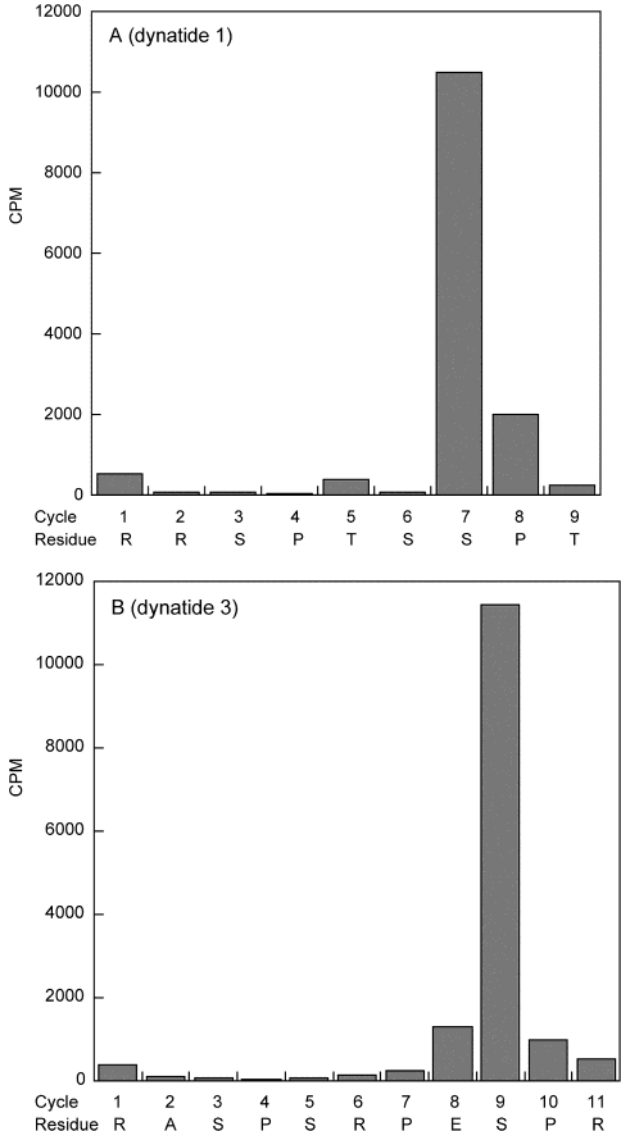

FIGURE 3: Determining the Mnb/Dyrk1A phosphorylation site in dynatides. Dynatides were phosphorylated with Mnb/Dyrk1A in the presence of [^{32}P]ATP and then subjected to manual Edman degradation as described in Materials and Methods. The radioactivity released in each cycle of degradation was plotted against the cycle. The amino acid residue corresponding to each cycle is indicated: (A) dynatide 1 and (B) dynatide 3.

masses indicated that S857 is phosphorylated as depicted in Figure 4B. These results indicate that S857 is phosphorylated at low kinase concentrations.

Dynamin 1 phosphorylated with a large dose of kinase (24 units of kinase/μg dynamin) was also analyzed. Again, S857 was phosphorylated, and S778 phosphorylation was not observed (Figure 5). Although phosphorylated A[785−796]R and R[784−796]R peptides were also absent in the MS spectrum, a new peptide at *m*/*z* 5195.7 corresponding to phosphorylated A[785−838]R was detected (Figure 5). This peptide is expected when trypsin skips R796, an indication that the neighboring S795 may be phosphorylated. Since peptide A[785−838]R was observed only when dynamin 1 was phosphorylated at a high Mnb/Dyrk1A concentration, it suggests that S795 phosphorylation requires high kinase concentrations.

Probing Mnb/Dyrk1A Phosphorylation at S795 and S857 with Phosphorylation Site-Specific Antibodies. Using Mnb/Dyrk1A-phosphorylated dynatide 3 as the antigen, a monoclonal antibody (3D3) specific for phosphorylated S857 was produced. 3D3 together with phosphorylated S795-specific antibody p-Dynamin I was used to investigate phosphorylation at S795 and S857 in full-length dynamin 1. Antibody 3D3 is highly selective for Mnb/Dyrk1A-phosphorylated dynatide 3 and dynamin 1, while it has no reactivity against their unphosphorylated counterparts (Figure 6A). It also exhibited no reactivity toward dynatide 1 or 2 regardless of the state of phosphorylation (data not shown). On the other hand, antibody p-Dynamin I recognized Mnb/Dyrk1A-phosphorylated dynatide 2 and dynamin 1 (Figure 6B) but not dynatide 1 or 3 (data not shown).

Using these antibodies, we first analyzed S795 and S857 phosphorylation with different kinase concentrations. Antibody 3D3 did not recognize purified rat dynamin 1 under the assay conditions; however, p-Dynamin I consistently produced a faint staining with the same sample (Figure 7B,D). The faint staining was attributed to the antibodies rather than to residual S795 phosphorylation because it could not be reduced by alkaline phosphatase treatment (data not shown). Therefore, both S795 and S857 were concluded to be unphosphorylated in our dynamin sample. This is not surprising because no measure was taken to inhibit phosphatases during dynamin 1 preparation. Upon incubation with low concentrations of Mnb/Dyrk1A, 3D3 reactivity quickly appeared and reached a plateau (Figure 7A). In contrast, p-Dynamin I reactivity was evident only when high concentrations of Mnb/Dyrk1A were used for phosphorylation (Figure 7B). These results are consistent with MS data showing that Mnb/Dyrk1A prefers S857 over S795. PKC was known to phosphorylate dynamin 1 at S795 (*34*); thus, PKC-phosphorylated dynamin 1 was also included in the assay. While p-Dynamin I reacted with the PKC-phosphorylated dynamin 1, 3D3 was unable to recognize the protein (Figure 7A,B). This result indicates that PKC phosphorylates dynamin 1 at S795 but not at S857.

We then selected a concentration of Mnb/Dyrk1A at which Mnb/Dyrk1A is capable of phosphorylating both residues and followed the time course of phosphorylation. Results in panels C and D of Figure 7 show that the reactivity for 3D3 reached its maximum level much earlier than that for p-Dynamin I. Again, the result indicates that S857 is the preferred phosphorylation site.

Effects of Site-Specific Mutations on Binding of Dynamin 1 to Endocytic Accessory Proteins. To determine whether phosphorylation directly alters the binding to endocytic accessory proteins, we examined dynamin 1aa variants harboring phosphorylation-mimicking mutation(s). Three mutants [S795E, S857E, and S795E/S857E double mutant (DE)] were constructed and analyzed. N-Terminally HA-tagged proteins were transiently expressed in Cos7 cells and verified by staining with two different anti-dynamin antibodies. Figure 8A showed that all dynamin constructs were expressed at similar levels in Cos7 cells. Unexpectedly, none of the expressed proteins reacted with the anti-HA tag antibody from two suppliers (data not shown). Therefore, Hudy-1 was used in all subsequent experiments for dynamin detection. The use of Hudy-1 will not impede the analysis because the level of endogenous dynamin 1 is diminishingly low compared to that of the overexpressed proteins (Figure 8A). To avoid potential complications associated with

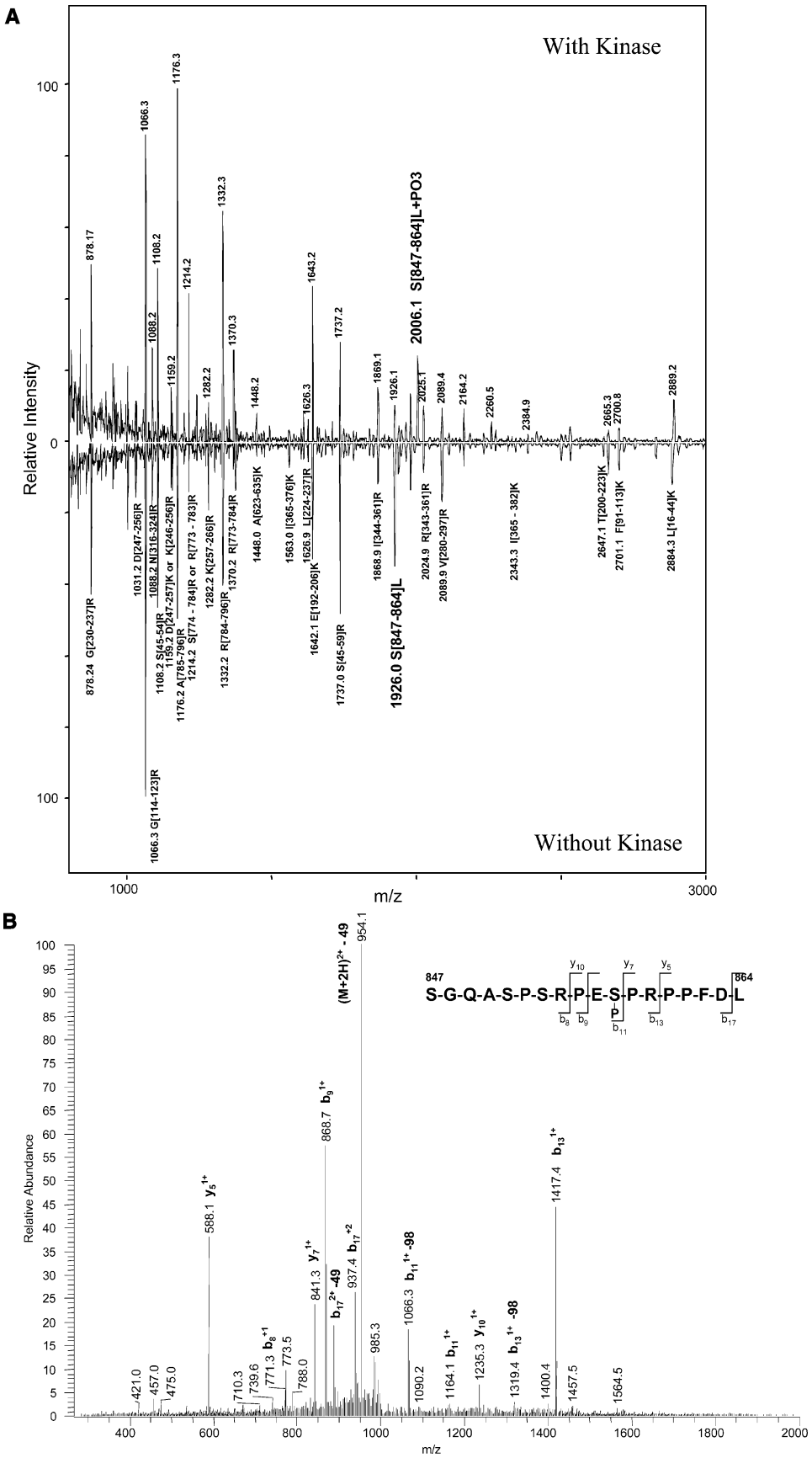

FIGURE 4: MALDI-TOF MS analysis of dynamin 1 phosphorylated by a low level of Mnb/Dyrk1A (A) and MS/MS analysis of the peptide at *m*/*z* 1003.1 (B). (A) Dynamin 1 was phosphorylated by Mnb/Dyrk1A (2 units/μg of dynamin) and then processed for MALDI-TOF MS analysis as described in Materials and Methods. Peptides containing S778, S795, S857, and many other dynamin fragments were labeled. (A) The *m*/*z* 1003.1 ion corresponding to the doubly charged ion of the *m*/*z* 2006.1 peptide identified in panel A was selected and subjected to MS/MS analysis as described in Materials and Methods. S857 phosphorylation was confirmed by the presence of various fragment ions generated from the phosphorylated S[847−864]L peptide.

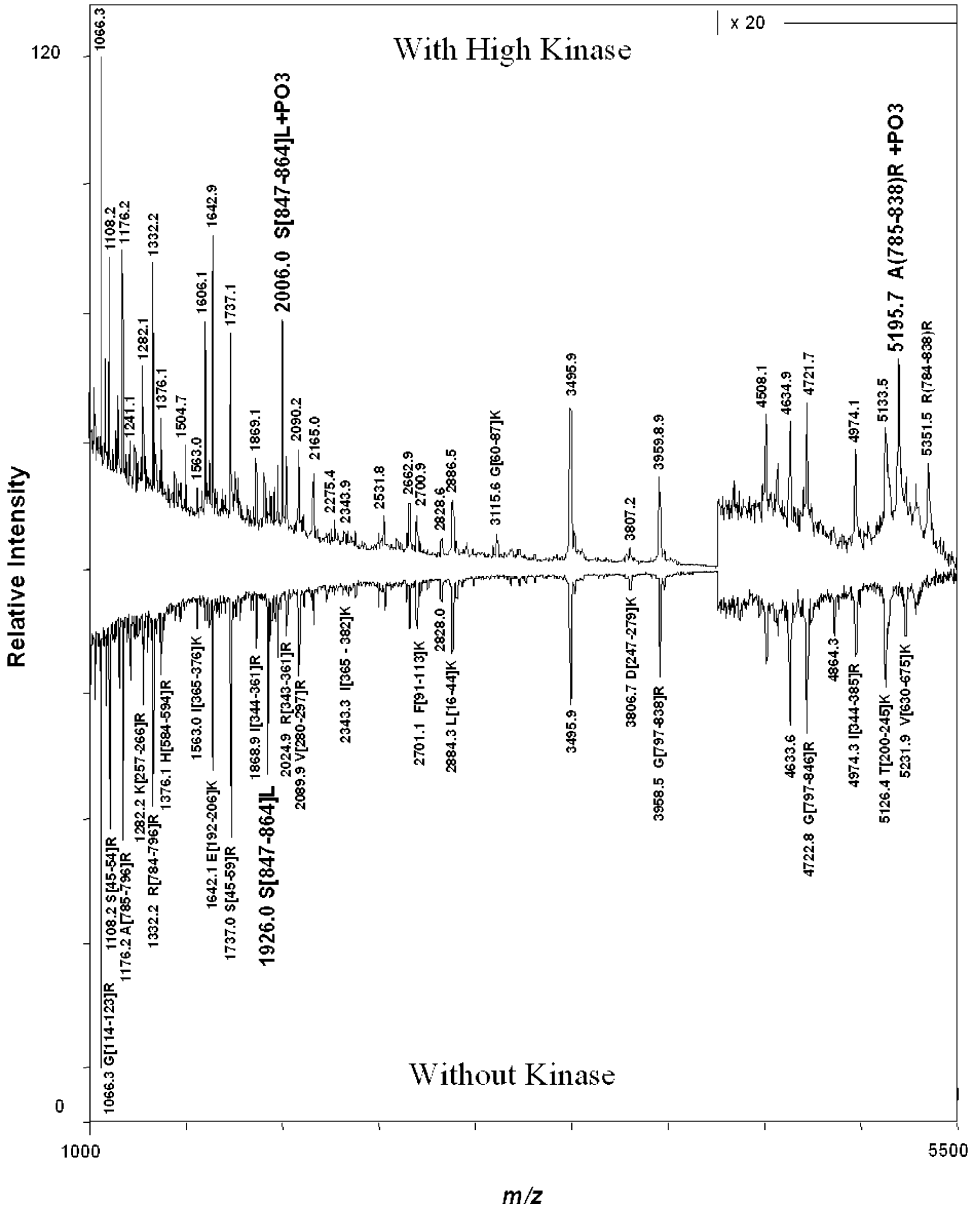

FIGURE 5: MALDI-TOF MS analysis of dynamin 1 phosphorylated by a high level of Mnb/Dyrk1A. Dynamin 1 was phosphorylated with Mnb/Dyrk1A at 24 units of kinase/μg of dynamin and analyzed by MALDI-TOF MS as described in the legend of Figure 4.

dynamin 1 phosphorylation at other sites, lysates were prepared without phosphatase inhibitors. The pull-down assay shows that wild-type (WT) dynamin 1aa is bound to amphiphysin 1 and Grb 2 under the assay conditions (Figure 8B,C). The binding to amphiphysin was nearly eliminated by the S857E mutation, while the same mutation enhanced the binding to Grb 2. These results support the conclusion that S857 phosphorylation causes both reduction of the level of binding to amphiphysin and enhancement of binding to Grb 2.

In contrast, the mutation simulating S795 phosphorylation (S795E) had little effect on binding of dynamin 1aa to amphiphysin and Grb 2 (Figure 8B,C). Interestingly, when the S795E mutation was combined with the S857E mutation (the DE mutant), it completely reversed the inhibitory effect of S857E on binding of dynamin 1aa to amphiphysin. This observation is in accord with the concentration-dependent biphasic effect of Mnb/Dyrk1A phosphorylation on dynamin 1−amphiphysin 1 binding (*12*). On the other hand, an additional S795E mutation was found to further enhance the binding of the S857E mutant to Grb 2. No biphasic effect was observed (Figure 8C).

Phosphorylation of S857 in Rat Brain Triton Extract (BTE) by the Endogenous Kinase. Incubating BTE with ATP and phosphatase inhibitors alters the binding of dynamin to amphiphysin 1 (*6*). To determine whether the same treatment produces S795 or S857 phosphorylation, extracts were treated (with ATP and phosphatase inhibitors) and analyzed with antibodies 3D3 and p-Dynamin I. The treatment promotes 3D3 staining of a 100 kDa protein (Figure 9A). To verify the identity of this 100 kDa protein, dynamin 1 was IP (with antibody C-16) from control and treated BTE and then reprobed with antibodies Hudy-1 and 3D3. Anti-dynamin 1 monoclonal antibody Hudy-1 (*35*) does not differentiate between unphosphorylated and Mnb/Dyrk1A-phosphorylated dynamin 1 (*12*). The staining showed that dynamin IP was equally efficient in control and treated samples (Figure 9B). In contrast, 3D3 stained dynamin 1 only from the treated extracts (Figure 9C). This confirmed that dynamin 1 is phosphorylated at S857 in treated crude brain extracts by

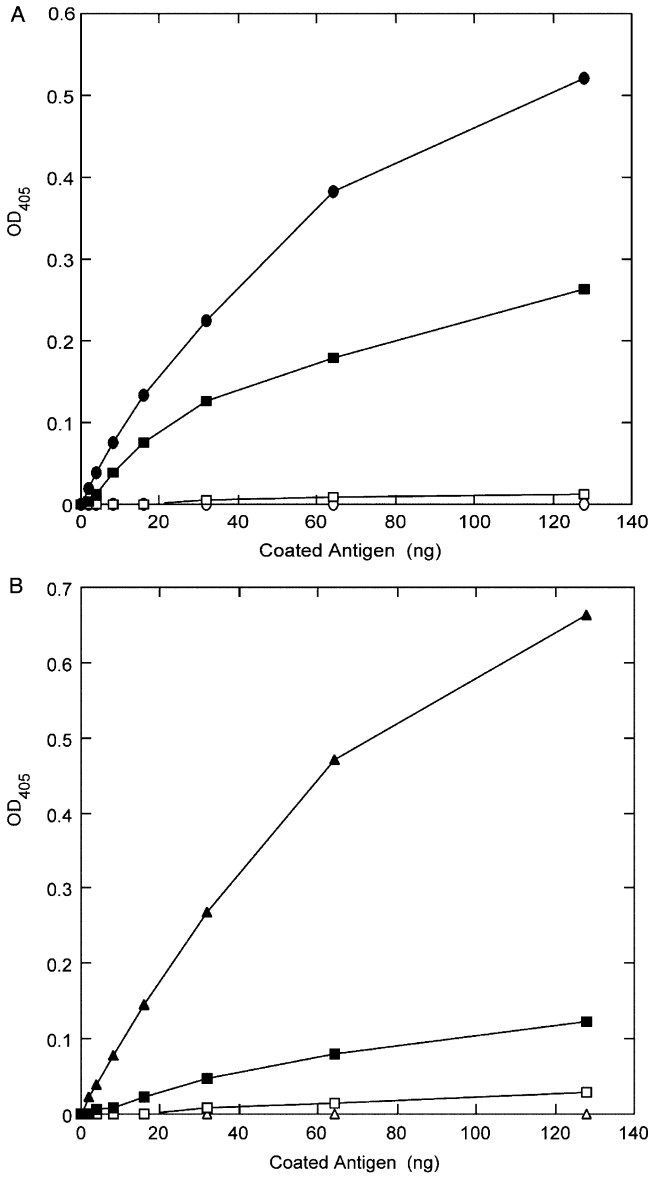

FIGURE 6: Specificity of antibodies 3D3 and p-Dynamin I. Antibody specificity was determined with an ELISA. Antigens were prepared by phosphorylating 1 μg of substrate with or without Mnb/Dyrk1A (24 units). ELISA plates were coated with 0−128 ng of antigen per well. The data used for plotting were the average of corrected (for *p*-nitrophenyl phosphate alone background) absorbance readings from three independent assays. Panel A shows data for antibody 3D3 and panel B for antibody p-Dynamin I: (▲) phosphorylated dynatide 2, (△) control dynatide 2, (●) phosphorylated dynatide 3, (○) control dynatide 3, (■) phosphorylated dynamin 1, and (□) control dynamin 1.

the endogenous kinase. On the other hand, the same treatment did not produce a signal with the antibody p-Dynamin I (Figure 9D). Since the assay was performed under the conditions in which antibodies 3D3 and p-Dynamin I were shown to generate similar signal strengths (Figure 7), the result indicates that S795 is not phosphorylated in BTE.

Phosphorylation and Dephosphorylation of Dynamin 1 at S857 in PC12 Cells. We subsequently examined dynamin 1xa phosphorylation at S795 and S857 in PC12 cells, which is known to express the dynamin 1xa isoform (*24*). The level of dynamin 1xa is low. To improve the detection, endogenous dynamin 1 was concentrated by IP (with immobilized antibody C-16) and then analyzed. The precipitated dynamin

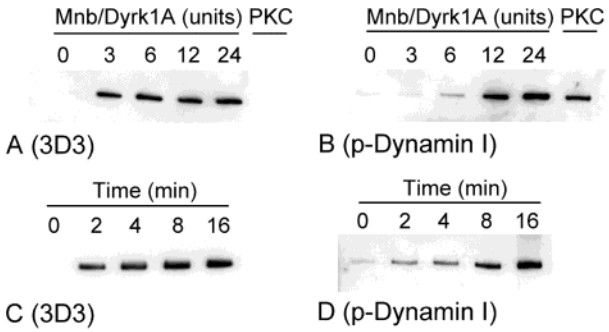

FIGURE 7: Mnb/Dyrk1A concentration-dependent (A and B) and time course (C and D) phosphorylation of S795 and S857. For the kinase concentration-dependent assay, dynamin 1 (1 μg) was phosphorylated with the indicated amounts of Mnb/Dyrk1A in solution for 30 min at 30 °C. For the time course assay, the ratio of 24 units of kinase/μg of dynamin 1 was used. The reaction was initiated by the addition of dynamin 1 and allowed to proceed at 30 °C. At the indicated times, an aliquot of the reaction mixture was withdrawn and the reaction terminated by boiling in SDS−PAGE loading buffer. All samples were loaded at 50 ng per lane: (A and C) 3D3 staining and (B and D) p-Dynamin I staining.

1 from undifferentiated PC12 cells cultured under the polarizing conditions (Figure 10A) was stained with antibody 3D3 (Figure 10B) but not with p-Dynamin 1 (Figure 10C). Again, we have performed the immunoblotting under the conditions as described in the legend of Figure 7. Our results suggest that S857 of dynamin 1xa, but not S795, is phosphorylated in PC12 cells under polarizing conditions. We then examined whether dynamin 1 S857 phosphorylation in PC12 cells could be stimulated to dephosphorylate by depolarizing the membranes. After incubation with 90 mM KCl, the level of S857 phosphorylation in PC12 cells was reduced by ∼46% without any effect on the protein levels of dynamin 1 (Figure 10D). This observation indicates that the state of S857 phosphorylation depends on membrane potentials. Similar results were obtained from NGF-differentiated PC12 cells (data not shown). We subsequently determined the effects of Mnb/Dyrk1A overexpression on dynamin 1xa S857 phosphorylation *in vivo*. PC12 cells were transfected with WT Mnb/Dyrk1A, and the endogenous dynamin 1xa was then analyzed with antibody 3D3. Results in Figure 11 show that expression vector pcMnb transfection leads to Mnb/Dyrk1A overproduction (Figure 11B), which in turn produces a moderate increase in the level of S857 phosphorylation (Figure 11A). The elevated level of S857 phosphorylation apparently requires Mnb/Dyrk1A activity because the kinase-deficient mutant (*11*, *12*) harboring both the Y319F and Y321F substitutions (DF) has no stimulating effect. However, the S857 phosphorylation enhancement (about 50%) is not directly proportional to overproduction of Mnb/Dyrk1A (>3-fold), suggesting that the endogenous dynamin 1xa is likely to be highly phosphorylated at S857 under our assay conditions.

DISCUSSION

On the basis of the stoichiometry of phosphate incorporation and its biphasic effect on binding of dynamin 1 to amphiphysin, we speculated earlier that Mnb/Dyrk1A differentially phosphorylated dynamin 1 at two sites with opposing outcomes (*12*); phosphorylation at the fast site is achieved with low kinase concentrations and leads to the reduction in the level of binding of amphiphysin, while

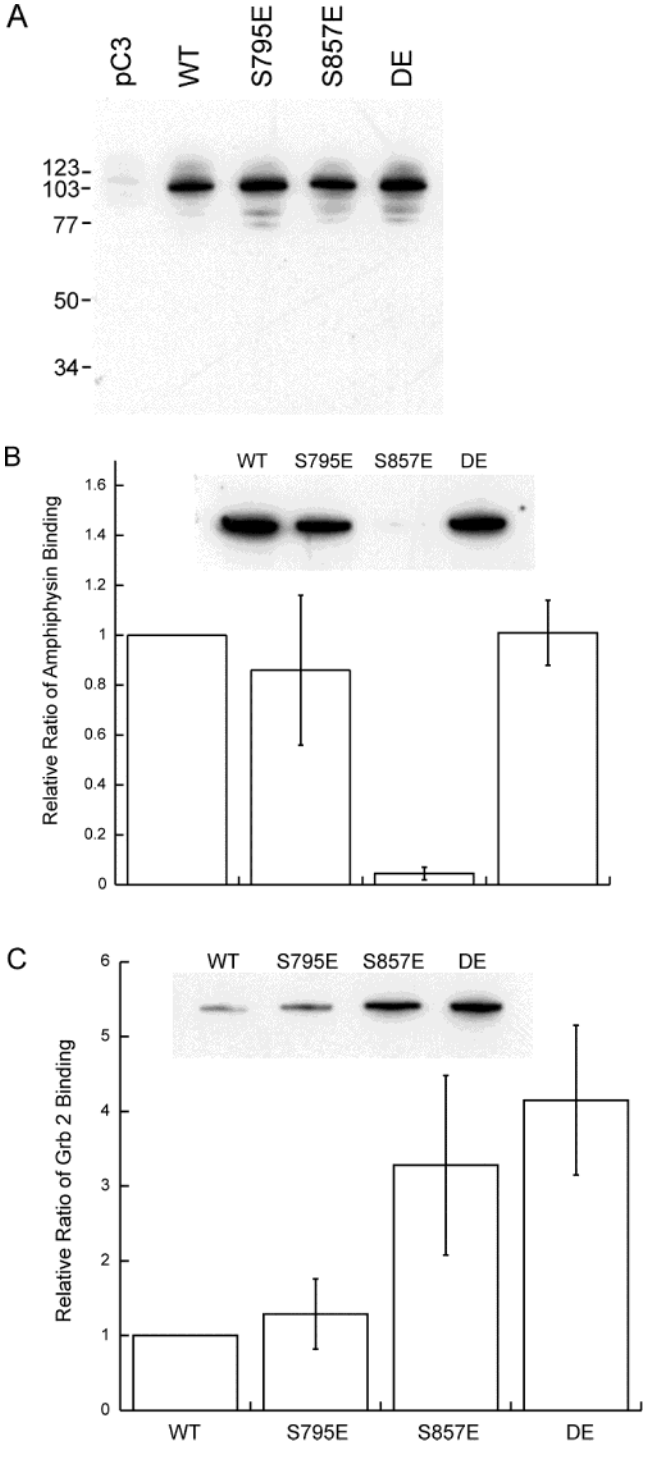

FIGURE 8: Expression and binding assay of dynamin 1aa mutants. (A) Expression of dynamins in Cos7 cells. Dynamin expression in transfected Cos7 cells (30 μg of total protein per lane) was analyzed by antibody Hudy-1 staining. Dynamin and mutants are labeled accordingly. PC3, transfected with pcDNA3, the cloning vector. (B) Amphiphysin 1 binding and (C) Grb 2 binding. The binding assay was performed by the pull-down assay as described in Materials and Methods. Plots showing the average of three independent trials (normalized to that for the wild type) with a typical binding result (insert) are presented. Amphiphysin 1 binding was deliberately overexposed to show the level of binding reduction for the S857E mutant.

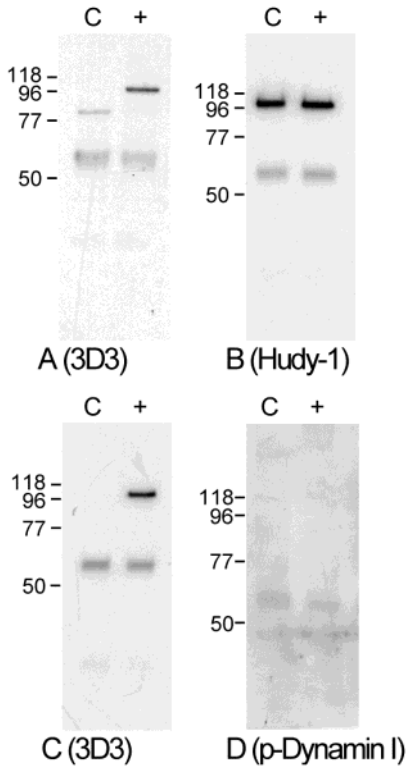

FIGURE 9: Phosphorylation of dynamin 1 at S857 in rat BTE. Extracts were prepared and treated as described in Materials and Methods. The control and treated samples (20 μg of total protein) were then probed with antibody 3D3 (A) or p-Dynamin I (D). To verify the identity of the stained 100 kDa protein, dynamin 1 in extracts was IP with the anti-dynamin antibody C-16 and then probed with antibodies Hudy-1 (B) and 3D3 (C): C, control; and +, treated with ATP and phosphatase inhibitors.

phosphorylation at the slow site, which is accomplished only with high kinase concentrations, counters the effects of the fast site phosphorylation. We have mapped the Mnb/Dyrk1A phosphorylation sites in dynamin 1 and provided several lines of evidence that support the hypothesis.

With denatured proteins and peptides, Mnb/Dyrk1A could phosphorylate S778, S795, and S857. However, only S795 phosphorylation and S857 phosphorylation were observed in the native protein analyzed by MS. Although phosphorylation at S778 cannot be completely ruled out by the negative MS results, the relative kinetic rates of phosphorylation at each site (Table 2 and Figure 7) suggest that S778 phosphorylation is miniscule. Since phosphorylation at S857 always precedes that at S795 under the various conditions that have been examined (Figures 4, 5, and 7), the data are consistent with S857 being the fast Mnb/Dyrk1A site *in vitro*. Phosphorylation at the slower S795 site is possible only when the reaction is performed with more kinase and/or for a longer duration (Figures 5 and 7). The reason that S857 is phosphorylated more readily than S795 may be because the sequence around S857 more closely resembles the consensus phosphorylation sequence. In addition, S857, which is near dynamin 1's C-terminus, may be more accessible to kinase than S795. S857 of dynamin 1 is phosphorylated in BTE as well as in PC 12 cells by the endogenous kinase (Figures 9 and 10). Significantly, the state of S857 phosphorylation is apparently dependent on membrane potentials (Figure 10) and the level of Mnb/Dyrk1A (Figure 11). These observations indicate that S857 phosphorylation is likely to be a physiological event and Mnb/Dyrk1A may be involved in phosphorylating S857 *in vivo*. On the other hand, the failure

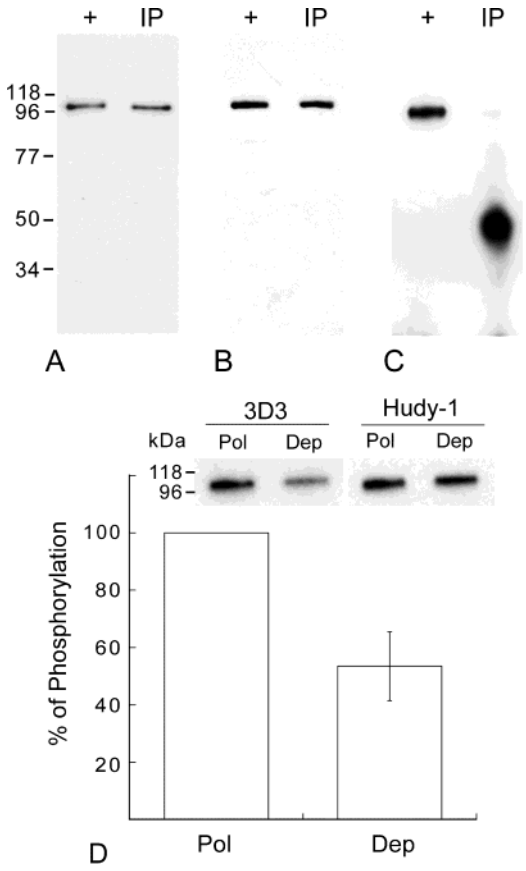

FIGURE 10: Phosphorylation and dephosphorylation of dynamin 1 at S857 in PC12 cells. Dynamin 1 in PC12 cells was IP from cell lysates with anti-dynamin 1 antibody C-16 and then analyzed for S857 and S795 phosphorylation by immunoblotting as described in Materials and Methods. A positive control (+) (dynamin 1 phosphorylated with a high Mnb/Dyrk1A concentration) was used together with precipitated proteins (IP) for staining with Hudy-1 (A), 3D3 (B), and p-Dynamin I (C). (D) S857 phosphorylation in polarized and depolarized PC12 cells. Polarized and depolarized PC12 cells were prepared in parallel except that depolarized cells were exposed to 90 mM K^+ ions. Dynamin 1 was similarly IP from cell lysates and first probed with 3D3, stripped, followed by Hudy-1 staining. The level of S857 phosphorylation under the depolarized conditions was calculated as described in Materials and Methods. Depolarization reduces the average level of phosphorylation to 53.5 ± 12.0% of the polarized cells based on four independent trials: Pol, polarized samples; and Dep, depolarized samples.

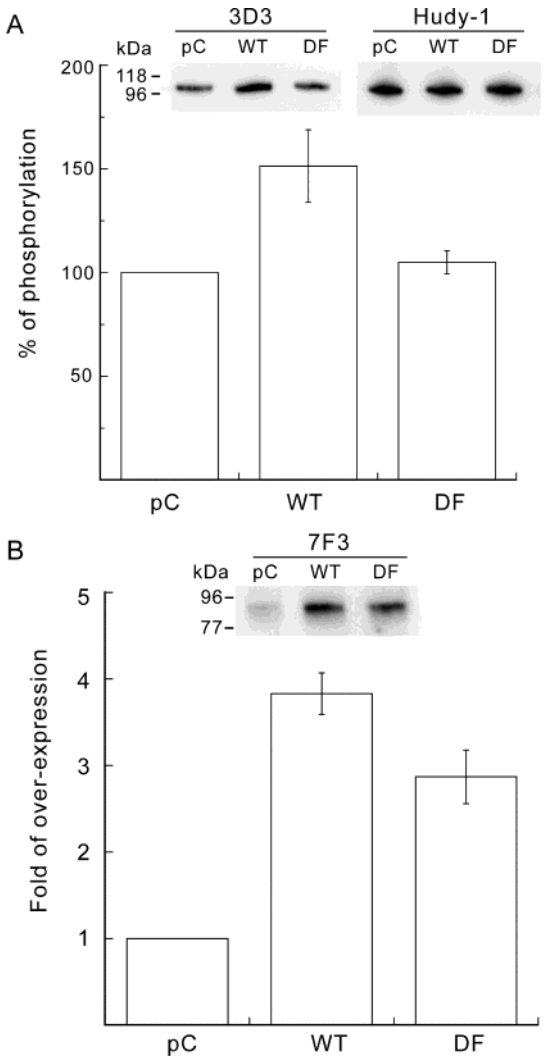

FIGURE 11: Effects of Mnb/Dyrk1A overexpression on the phosphorylation of dynamin 1xa at S857. (A) Level of S857 phosphorylation. PC12 cells were transfected with either pcDNA3 (pC), pcMnb (WT), or pcMnb harboring Y319F and Y321F mutations (DF) and maintained under polarizing conditions. Dynamin 1 was extracted from transfected cells, IP, and analyzed for S857 phosphorylation in a manner similar to that described in the legend of Figure 10. The data were corrected for the level of dynamin 1 (Hudy-1 staining) before plotting. The plot represents the average of three independent trials for each transfection (normalized to pC). (B) Mnb/Dyk1A overproduction in transfected PC12 cells. Mnb/Dyrk1A was detected directly in crude cell lysates (20 μg of total protein) by immunoblotting using antibody 7F3. The average of three independent trials is shown in the plot (normalized to pC).

to detect S795 phosphorylation in both BTE and PC12 cells suggests that S795 phosphorylation as assessed *in vitro* may not occur *in vivo*.

The results of site-specific S857E mutants offer direct evidence that supports the conclusion that the fast site S857 phosphorylation causes the reduction in the level of binding of dynamin 1 to amphiphysin 1 (Figure 8B). S857 phosphorylation also directly contributes to the enhanced Grb 2 binding (Figure 8C). In contrast, the mutation that simulated the slow site phosphorylation, S795E, caused no significant changes in binding to amphiphysin or Grb 2 (Figure 8). However, it could fully reverse the weak amphiphysin 1 binding associated with the S857E mutation. Clearly, the biphasic switchover is caused by the progression from the singly phosphorylated state to the doubly phosphorylated state. Although a highly phosphorylated dynamin 1 was found to have an enhanced amphiphysin binding activity, this activity was not observed on the DE mutant. This may be due to the limitation of serine-to-glutamate substitution in fully simulating phosphorylation. Apparently, the binding of dynamin 1 to amphiphysin can be regulated via multiple ways, as Cdk5 phosphorylation was recently shown to inhibit the binding by phosphorylating dynamin at T780 (*10*). Paradoxically, the same kinase was also found to phosphorylate S774 along with S778 but to exert no inhibitory effect on dynamin 1−ampiphysin 1 binding in another study (*9*).

Studies have localized the amphiphysin 1 binding domain to a single region of dynamin 1 (residues 831−838) (*36*, *37*). In addition to residues 831−838, Grb 2 may also need residues 778−795 and 813−818 of dynamin 1 for binding (*38*−*40*). All these regions contain a polyproline-2 helix, the SH3 domain binding ligand (*41*). The involvement of different regions may explain why the same phosphorylation causes an opposite effect on binding to amphiphysin and Grb

2. Showing how phosphorylation at S857 and S795 affects the access of SH3 domain-containing proteins to the PRD requires an understanding of PRD structures, which are yet to be defined. Regardless, the fact that Mnb/Dyrk1A phosphorylation can enhance the binding to one protein while inhibiting the binding of another suggests that Mnb/Dyrk1A may play a role in controlling the participation of dynamin 1 in different cellular pathways.

The sequence around S857 is unique to the dynamin 1xa variants (*23*, *24*). The identification of S857 as the major Mnb/Dyrk1A phosphorylation site suggests that Mnb/Dyrk1A is limited in its activity to dynamin 1xa isoforms. Both dynamin 1xa (*36*, *42*) and Mnb/Dyrk1A (*14*−*16*, *43*−*45*) are strongly expressed in various brain regions. Although the direct evidence is lacking, it will not be surprising if their distributions overlap. In fact, dynamin 1 and Mnb/Dyrk1A have been colocalized in growing dendrites of developing chicken Purkinje cells (*46*); this finding supports the notion that they are potential functional partners. Mnb/Dyrk1A contains a bipartite nuclear targeting sequence (*11*), which has been shown to deliver the protein to nucleus when overexpressed (*47*, *48*). However, a substantial portion of the endogenous Mnb/Dyrk1A is found in cytosolic compartments, such as neuronal processes and synapes, of mouse (*45*), chicken (*46*), and human (*30*) central nervous systems. This pattern of subcellular distribution may explain why Mnb/Dyrk1A phosphorylates nuclear proteins such as FKHR (*49*) as well as cytosolic proteins like dynamin 1. It should be pointed out that Mnb/Dyrk1A was previously shown to phosphorylate dynamin 1ab and dynamin 2 isoforms in a solid-phase assay (*12*). These two isoforms do not contain S857 and are unlikely to be Mnb/Dyrk1A substrates. This apparent discrepancy may be due to the use of denatured proteins in the solid-phase assay, which may expose the nonphysiological site(s) for phosphorylation.

Phosphorylation was proposed to regulate the recruitment of dynamin 1 to functional complexes through the interaction of PRD and endocytic accessory proteins (*2*, *6*). Our findings that the endogenous kinase phosphorylates S857 and modifies the binding of dynamin to endocytic accessory proteins strongly support a role for phosphorylation in controlling dynamin complex assembly. The findings also suggest that Mnb/Dyrk1A is a candidate kinase that is likely to be involved in this process. Clearly, dynamin 1 is also phosphorylated and regulated by other kinases (*7*−*10*). These phosphorylations may happen in concert to promote the complex behavior of dynamin 1. S795 is not normally phosphorylated, but the situation may change if the level of Mnb/Dyrk1A is increased (Figure 7). Mnb/Dyrk1A expression is enhanced in Down's syndrome (*19*, *20*). Whether enhanced Mnb/Dyrk1A expression could lead to aberrant dynamin 1 phosphorylation and a change in its activity will be interesting to explore.

ACKNOWLEDGMENT

We are indebted to Mr. James C. M. Chen and Ms. Heni Hong of Institute for Basic Research's monoclonal antibody core facility for producing antibodies 3D3 and 7F3. We thank Dr. Thomas C. Südhof of Howard Hughes Medical Institute at the University of Texas Southwestern Medical Center (Dallas, TX) for providing dynamin clones pCMV96-7. We also thank Drs. Carl Dobkin, Robert Denman, Robert Gould, David Miller, and Song-Yu Yang for their comments on the manuscript.

REFERENCES

1. Schmid, S. L., McNiven, M. A., and De Camilli, P. (1998) Dynamin and its partners: a progress report, *Curr. Opin. Cell Biol. 10*, 504−512.
2. Slepnev, V. I., and De Camilli, P. (2000) Accessory factors in clathrin-dependent synaptic vesicle endocytosis, *Nat. Rev. Neurosci. 1*, 161−172.
3. Conner, S. D., and Schmid, S. L. (2003) Regulated portals of entry into the cell, *Nature 422*, 37−44.
4. Robinson, P. J., Hauptschein, R., Lovenberg, W., and Dunkley, P. R. (1987) Dephosphorylation of synaptosomal proteins P96 and P139 is regulated by both depolarization and calcium, but not by a rise in cytosolic calcium alone, *J. Neurochem. 48*, 187−195.
5. Robinson, P. J., Sontag, J. M., Liu, J. P., Fykse, E. M., Slaughter, C., McMahon, H., and Südhof, T. C. (1993) Dynamin GTPase regulated by protein kinase C phosphorylation in nerve terminals, *Nature 365*, 163−166.
6. Slepnev, V. I., Ochoa, G. C., Butler, M. H., Grabs, D., and De Camilli, P. (1998) Role of phosphorylation in regulation of the assembly of endocytic coat complexes, *Science 281*, 821−824.
7. Earnest, S., Khokhlatchev, A., Albanesi, J. P., and Barylko, B. (1996) Phosphorylation of dynamin by ERK2 inhibits the dynamin-microtubule interaction, *FEBS Lett. 396*, 62−66.
8. Ahn, S., Maudsley, S., Luttrell, L. M., Lefkowitz, R. J., and Daaka, Y. (1999) Src-mediated tyrosine phosphorylation of dynamin is required for β2-adrenergic receptor internalization and mitogen-activated protein kinase signaling, *J. Biol. Chem. 274*, 1185−1188.
9. Tan, T. C., Valova, V. A., Malladi, C. S., Graham, M. E., Berven, L. A., Jupp, O. J., Hansra, G., McClure, S. J., Sarcevic, B., Boadle, R. A., Larsen, M. R., Cousin, M. A., and Robinson, P. J. (2003) Cdk5 is essential for synaptic vesicle endocytosis, *Nat. Cell Biol. 5*, 701−710.
10. Tomizawa, K., Sunada, S., Lu, Y. F., Oda, Y., Kinuta, M., Ohshima, T., Saito, T., Wei, F. Y., Matsushita, M., Li, S. T., Tsutsui, K., Hisanaga, S., Mikoshiba, K., Takei, K., and Matsui, H. (2003) Cophosphorylation of amphiphysin I and dynamin I by Cdk5 regulates clathrin-mediated endocytosis of synaptic vesicles, *J. Cell Biol. 163*, 813−824.
11. Kentrup, H., Becker, W., Heukelbach, J., Wilmes, A., Schürmann, A., Huppertz, C., Kainulainen, H., and Joost, H. G. (1996) Dyrk, a dual specificity protein kinase with unique structural features whose activity is dependent on tyrosine residues between subdomains VII and VIII, *J. Biol. Chem. 271*, 3488−3495.
12. Chen-Hwang, M. C., Chen, H. R., Elzinga, M., and Hwang, Y. W. (2002) Dynamin is a minibrain kinase/dual specificity Yak1-related kinase 1A substrate, *J. Biol. Chem. 277*, 17597−17604.
13. Tejedor, F., Zhu, X. R., Kaltenbach, E., Ackermann, A., Baumann, A., Canal, I., Heisenberg, M., Fischbach, K. F., and Pongs, O. (1995) minibrain: a new protein kinase family involved in postembryonic neurogenesis in *Drosophila*, *Neuron 14*, 287−301.
14. Shindoh, N., Kudoh, J., Maeda, H., Yamaki, A., Minoshima, S., Shimizu, Y., and Shimizu, N. (1996) Cloning of a human homolog of the *Drosophila* minibrain/rat Dyrk gene from the Down syndrome critical region of chromosome 21, *Biochem. Biophys. Res. Commun. 225*, 92−99.
15. Guimerá, J., Casas, C., Pucharcòs, C., Solans, A., Domènech, A., Planas, A. M., Ashley, J., Lovett, M., Estivill, X., and Pritchard, M. A. (1996) A human homologue of *Drosophila* minibrain (MNB) is expressed in the neuronal regions affected in Down syndrome and maps to the critical region, *Hum. Mol. Genet. 5*, 1305−1310.
16. Song, W. J., Sternberg, L. R., Kasten-Sportès, C., Van Keuren, M. L., Chung, S. H., Slack, A., Miller, D. E., Glover, T. W., Chiang, P. W., Lou, L., and Kurnit, D. M. (1996) Isolation of human and murine homologues of the *Drosophila* minibrain gene: human homologue maps to 21q22.2 in the Down syndrome "critical region", *Genomics 38*, 331−339.
17. Ohira, M., Seki, N., Nagase, T., Suzuki, E., Nomura, N., Ohara, O., Hattori, M., Sakaki, Y., Eki, T., Murakami, Y., Saito, T., Ichikawa, H., and Ohki, M. (1997) Gene identification in 1.6-Mb region of the Down syndrome region on chromosome 21, *Genome Res. 7*, 47−58.

18. Chen, H., and Antonarakis, S. E. (1997) Localisation of a human homologue of the *Drosophila* mnb and rat Dyrk genes to chromosome 21q22.2, *Hum. Genet. 99*, 262−265.
19. Guimerá, J., Casas, C., Estivill, X., and Pritchard, M. (1999) Human minibrain homologue (MNBH/DYRK1): characterization, alternative splicing, differential tissue expression, and overexpression in Down syndrome, *Genomics 57*, 407−418.
20. Tassone, F., Lucas, R., Slavov, D., Kavsan, V., Crnic, L., and Gardiner, K. (1999) Gene expression relevant to Down syndrome: problems and approaches, *J. Neural. Transm. Suppl. 57*, 179−195.
21. Smith, D. J., and Rubin, E. M. (1997) Functional screening and complex traits: human 21q22.2 sequences affecting learning in mice, *Hum. Mol. Genet. 6*, 1729−1733.
22. Altafaj, X., Dierssen, M., Baamonde, C., Martí, E., Visa, J., Guimerá, J., Oset, M., González, J. R., Flórez, J., Fillat, C., and Estivill, X. (2001) Neurodevelopmental delay, motor abnormalities and cognitive deficits in transgenic mice overexpressing Dyrk1A (minibrain), a murine model of Down's syndrome, *Hum. Mol. Genet. 10*, 1915−1923.
23. Sontag, J. M., Fykse, E. M., Ushkaryov, Y., Liu, J. P., Robinson, P. J., and Südhof, T. C. (1994) Differential expression and regulation of multiple dynamins, *J. Biol. Chem. 269*, 4547−4554.
24. Cao, H., Garcia, F., and McNiven, M. A. (1998) Differential Distribution of Dynamin Isoforms in Mammalian Cells, *Mol. Biol. Cell 9*, 2595−2609.
25. Sung, Y. J., Carter, M., Zhong, J. M., and Hwang, Y. W. (1995) Mutagenesis of the H-ras p21 at glycine-60 residue disrupts GTP-induced conformational change, *Biochemistry 34*, 3470−3477.
26. Hwang, Y. W., Zhong, J. M., Poullet, P., and Parmeggiani, A. (1993) Inhibition of SDC25 C-domain-induced guanine-nucleotide exchange by guanine ring binding domain mutants of v-H-*ras*, *J. Biol. Chem. 268*, 24692−24698.
27. Casnellie, J. E. (1991) Assay of protein kinases using peptides with basic residues for phosphocellulose binding, *Methods Enzymol. 200*, 115−120.
28. Harlow, E., and Lane, D. (1988) *Antibodies, a laboratory manual*, Cold Spring Harbor Laboratory Press, Cold Spring Harbor, NY.
29. Ruegg, U. T., and Rudinger, J. (1977) Reductive cleavage of cystine disulfides with tributylphosphine, *Methods Enzymol. 47*, 111−116.
30. Wegiel, J., Kuchna, I., Nowicki, K., Frackowiak, J., Dowjat, K., Silverman, W. P., Reisberg, B., DeLeon, M., Wisniewski, T., Adayev, T., Chen-Hwang, M. C., and Hwang, Y. W. (2004) Cell type- and brain structure-specific patterns of distribution of minibrain kinase in human brain, *Brain Res. 1010*, 69−80.
31. Hunter, T., and Sefton, B. M. (1980) Transforming gene product of Rous sarcoma virus phosphorylates tyrosine, *Proc. Natl. Acad. Sci. U.S.A. 77*, 1311−1315.
32. Sullivan, S., and Wong, T. W. (1991) A manual sequencing method for identification of phosphorylated amino acids in phosphopeptides, *Anal. Biochem. 197*, 65−68.
33. Himpel, S., Tegge, W., Frank, R., Leder, S., Joost, H. G., and Becker, W. (2000) Specificity determinants of substrate recognition by the protein kinase DYRK1A, *J. Biol. Chem. 275*, 2431−2438.
34. Powell, K. A., Valova, V. A., Malladi, C. S., Jensen, O. N., Larsen, M. R., and Robinson, P. J. (2000) Phosphorylation of dynamin I on Ser-795 by protein kinase C blocks its association with phospholipids, *J. Biol. Chem. 275*, 11610−11617.
35. Warnock, D. E., Terlecky, L. J., and Schmid, S. L. (1995) Dynamin GTPase is stimulated by crosslinking through the C-terminal proline-rich domain, *EMBO J. 14*, 1322−1328.
36. Okamoto, P. M., Herskovits, J. S., and Vallee, R. B. (1997) Role of the basic, proline-rich region of dynamin in Src homology 3 domain binding and endocytosis, *J. Biol. Chem. 272*, 11629−11635.
37. Grabs, D., Slepnev, V. I., Songyang, Z., David, C., Lynch, M., Cantley, L. C., and De Camilli, P. (1997) The SH3 domain of amphiphysin binds the proline-rich domain of dynamin at a single site that defines a new SH3 binding consensus sequence, *J. Biol. Chem. 272*, 13419−13425.
38. Ando, A., Yonezawa, K., Gout, I., Nakata, T., Ueda, H., Hara, K., Kitamura, Y., Noda, Y., Takenawa, T., Hirokawa, N., Waterfield, M. D., and Kasuga, M. (1994) A complex of GRB2-dynamin binds to tyrosine-phosphorylated insulin receptor substrate-1 after insulin treatment, *EMBO J. 13*, 3033−3038.
39. Gout, I., Dhand, R., Hiles, I. D., Fry, M. J., Panayotou, G., Das, P., Truong, O., Totty, N. F., Hsuan, J., Booker, G. W., Campbell, I. D., and Waterfield, M. D. (1993) The GTPase dynamin binds to and is activated by a subset of SH3 domains, *Cell 75*, 25−36.
40. Seedorf, K., Kostka, G., Lammers, R., Bashkin, P., Daly, R., Burgess, W. H., van der Bliek, A. M., Schlessinger, J., and Ullrich, A. (1994) Dynamin binds to SH3 domains of phospholipase C gamma and GRB-2, *J. Biol. Chem. 269*, 16009−16014.
41. Yu, H., Chen, J. K., Feng, S., Dalgarno, D. C., Brauer, A. W., and Schreiber, S. L. (1994) Structural basis for the binding of proline-rich peptides to SH3 domains, *Cell 76*, 933−945.
42. Faire, K., Trent, F., Tepper, J. M., and Bonder, E. M. (1992) Analysis of dynamin isoforms in mammalian brain: dynamin-1 expression is spatially and temporally regulated during postnatal development, *Proc. Natl. Acad. Sci. U.S.A. 89*, 8376−8380.
43. Okui, M., Ide, T., Morita, K., Funakoshi, E., Ito, F., Ogita, K., Yoneda, Y., Kudoh, J., and Shimizu, N. (1999) High-level expression of the Mnb/Dyrk1A gene in brain and heart during rat early development, *Genomics 62*, 165−171.
44. Rahmani, Z., Lopes, C., Rachidi, M., and Delabar, J. M. (1998) Expression of the mnb (dyrk) protein in adult and embryonic mouse tissues, *Biochem. Biophys. Res. Commun. 253*, 514−518.
45. Marti, E., Altafaj, X., Dierssen, M., de la Luna, S., Fotaki, V., Alvarez, M., Perez-Riba, M., Ferrer, I., and Estivill, X. (2003) Dyrk1A expression pattern supports specific roles of this kinase in the adult central nervous system, *Brain Res. 964*, 250−263.
46. Hämmerle, B., Carnicero, A., Elizalde, C., Ceron, J., Martínez, S., and Tejedor, F. J. (2003) Expression patterns and subcellular localization of the Down syndrome candidate protein MNB/DYRK1A suggest a role in late neuronal differentiation, *Eur. J. Neurosci. 17*, 2277−2286.
47. Song, W. J., Chung, S. H., and Kurnit, D. M. (1997) The murine Dyrk protein maps to chromosome 16, localizes to the nucleus, and can form multimers, *Biochem. Biophys. Res. Commun. 231*, 640−644.
48. Becker, W., Weber, Y., Wetzel, K., Eirmbter, K., Tejedor, F. J., and Joost, H. G. (1998) Sequence characteristics, subcellular localization, and substrate specificity of DYRK-related kinases, a novel family of dual specificity protein kinases, *J. Biol. Chem. 273*, 25893−25902.
49. Woods, Y. L., Rena, G., Morrice, N., Barthel, A., Becker, W., Guo, S., Unterman, T. G., and Cohen, P. (2001) The kinase DYRK1A phosphorylates the transcription factor FKHR at Ser329 in vitro, a novel in vivo phosphorylation site, *Biochem. J. 355*, 597−607.

BI036060+